# Contributions of a Highly Conserved $V_H/V_L$ Hydrogen Bonding Interaction to scFv Folding Stability and Refolding Efficiency

Philip H. Tan,* Brenda M. Sandmaier,# and Patrick S. Stayton*

*Department of Bioengineering, University of Washington, Seattle 98195, and #Transplantation Biology Program, Clinical Research Division, Fred Hutchinson Cancer Center, Seattle, Washington 98104 USA

ABSTRACT The assembly of single-chain Fv (scFv) antibody fragments, consisting of an interconnected variable heavy chain ($V_H$) and variable light chain ($V_L$), is a cooperative process that requires coupled folding and domain association. We report here an initial investigation of $V_H/V_L$ domain-domain assembly with a site-directed mutagenesis study that probes a highly conserved $V_H/V_L$ hydrogen bonding interaction. $Gln^{168}$ of the S5 scFv (Kabat $V_H$ 39) is absolutely conserved in 95% of all $V_H$, and $Gln^{44}$ (Kabat $V_L$ 38) is found in 94% of all $\kappa$ $V_L$ (Glx in 95% of all $\lambda$ $V_L$). These side chains form two hydrogen bonds in head-to-tail alignment across the $V_H/V_L$ interface. Double mutant cycles at $Gln^{168}$ and $Gln^{44}$ were constructed to first investigate their contributions to thermodynamic folding stability, second to investigate whether stability can be improved, and third to determine whether refolding efficiencies are affected by mutations at these positions. The results demonstrate that the $Gln^{168}$-$Gln^{44}$ interaction is not a key determinant of S5 scFv folding stability, as sequential modification to alanine has no significant effect on the free energy of folding. Several mutations that alter the glutamines to methionine or charged amino acids significantly increase the thermodynamic stability by increasing the $m_g$ associated with the unfolding isotherm. These effects are hypothesized to arise largely from an increase in the $V_H/V_L$ association free energy that leads to tighter coupling between domain-domain association and folding. All of the mutants also display a reduced antigen binding affinity. Single and double methionine mutants also displayed significant increases in refolding efficiency of 2.4- to 3-fold over the native scFv, whereas the double alanine/methionine mutants displayed moderate 1.9- to 2.4-fold enhancement. The results suggest that reengineering the $V_H/V_L$ interface could be useful in improving the stability of single-chain antibodies, as Ala/Met mutations at these conserved positions increase the free energy of folding by 46% while minimally perturbing binding affinity. They also could be useful in improving scFv recovery from inclusion bodies as the mutations increase the refolding efficiency by more than twofold.

## INTRODUCTION

The protein folding problem has largely been approached from the perspective of small, discrete folding units or subunits. The next level of organization, domain-domain assembly, remains an important challenge for which much less detailed kinetic and thermodynamic characterization exists. It is interesting to note, for example, that many dimeric proteins are characterized by an apparent two-state folding equilibrium (Neet and Timm, 1994; Sauer et al., 1996). This implies a highly cooperative assembly process, but the molecular mechanisms by which individual domain folding is coupled to domain-domain association are poorly understood. The IgG antibody family is a good example in which global protein folding is coupled to domain association. The $F_{AB}'$ fragment requires the folding of the $V_H$ and $C_{H1}$ of the heavy chain and the $V_L$ and $C_L$ of the light chain, along with association across the $V_H/V_L$ and $C_{H1}/C_L$ interfaces. Equilibrium and kinetic studies of $F_{AB}'$ and subunits of $F_{AB}'$ have demonstrated the coupling of folding to domain association and the coupling of $V_H/V_L$ interactions and $C_{H1}/C_L$ interactions (Rowe and Tanford, 1973; Rowe, 1976; Hochman et al., 1976; Klein et al., 1979; Horne et al., 1982; Tsunenaga et al., 1987). Recent kinetic studies by Lilie et al. (1995) have supported a $F_{AB}'$ folding scheme that is initiated by the fast folding of individual domains coupled to domain-domain association, with subsequent formation of folding intermediates differing in prolyl isomerization and potentially in specific interface contacts.

Single-chain Fv antibodies (scFv) represent another interesting model system for studying domain-domain assembly. scFv antibodies are genetically engineered antibody fragments consisting of the variable heavy and variable light domains of intact monoclonal antibodies, connected through a synthetic linker of ~15 amino acids (Bird et al., 1988). The study of domain-domain assembly in the scFv model system reduces the complexity of the $F_{AB}'$ system to two interconnected folding units and one association interface. Because the folding and the association of the variable domains at the $V_H/V_L$ interface are structurally coupled to the $C_{H1}/C_L$ interface in nature, it is unclear whether the isolated scFv $V_H/V_L$ domains and interface are optimized in terms of folding stability and mechanism. The study of domain-domain assembly in the scFv model system could thus potentially provide designs that improve the scFv for technological applications. The scFv are widely considered to be relatively unstable, and in the few reported cases in which thermodynamic stability has been measured, the folding free energy is indeed small. Pantoliano et al. (1991) have studied the equilibrium unfolding of a fluorescein-

*Received for publication 16 January 1998 and in final form 2 June 1998.*

Address reprint requests to Dr. Patrick S. Stayton, Department of Bioengineering, Box 357962, University of Washington, Seattle, WA 98195. Tel.: 206-685-8148; Fax: 206-685-8256; E-mail: stayton@bioeng.washington.edu.



0006-3495/98/09/1473/10 $2.00

binding scFv, and reported the thermodynamic effects of derivatives differing in the length of the interconnecting linker. They observed a two-state unfolding transition with a folding free energy of 4.33 kcal/mol for the anti-fluorescein scFv. Voss and co-workers have similarly observed a two-state unfolding transition with an anti-ssDNA scFv, and obtained a folding free energy of just 1.44 kcal/mol (Gulliver et al., 1995). Interestingly, the grafting of heavy-chain CDR loops from the fluorescein-binding scFv to the anti-ssDNA scFv led to a substantial increase in the folding stability of the latter scFv. A mechanistic study of scFv fragment folding by Freund et al. (1996) has provided the first detailed kinetic characterization and provides evidence for the formation of a folding intermediate varying in prolyl isomerization. Other studies have shown that engineered disulfide linkages and chemical cross-linking across the $V_H$-$V_L$ interface can significantly increase the thermal stability of Fv antibodies and provide important routes for improved refolding properties (Glockshuber et al., 1990; Reiter et al., 1994).

We report here an initial site-directed mutagenesis and thermodynamic and refolding efficiency study of the scFv $V_H/V_L$ interface. Double mutant cycles have been constructed at a highly conserved hydrogen bonding pair, formed between glutamine 44 (Kabat $V_L$ 38) and glutamine 168 (Kabat $V_H$ 39) (Kabat et al., 1991; Chothia et al., 1985). The glutamine of the heavy chain is conserved in 95% of all heavy chain classes, whereas the glutamine of the light chain is 95% conserved in all $\kappa$ light chains and found as Glx in 95% of $\lambda$ light chains (Kabat et al., 1991). The two amide groups are aligned head to tail with respect to the amino and carbonyl functionalities, forming two hydrogen bonds that close the hydrophobic zipper of the highly conserved $V_H/V_L$ interface.

## MATERIALS AND METHODS

### Materials

All oligonucleotides for mutagenesis work were purchased from Integrated DNA Technologies (Coralville, IA). Most chemicals were purchased from Sigma (St. Louis, MO) or ICN (Costa Mesa, CA). All restriction endonucleases were purchased from New England Biolabs (Beverly, MA).

### Molecular modeling of S5 scFv structure

A search of the Swiss-Protein database resulted in a high sequence alignment fit to the McPC603 antibody (Satow et al., 1986). The S5 scFv had 67% exact match $V_H$ alignment (93% conservative match) and 69% exact match $V_L$ alignment (92% conservative match) to McPc603. This close sequence homology allowed the construction of a three-dimensional model of S5 using the software package Homology (Biosym, San Diego, CA). Briefly, the two sequences were aligned, and coordinates from McPc603 were transferred to S5 scFv, while coordinates for the linker were assigned by random search for the lowest energy conformation. The structure was then relaxed with the Discover program (InsightII, Biosym) by selective minimization of all atoms of the CDR loops and the side chains in the framework residues that were replaced. The backbone atoms of the framework were not minimized because of the close identity and conservation between McPC603 and S5 (Chothia and Lesk, 1986).

### Construction of interface mutant

The cloning of the $V_L$ and $V_H$ genes and the construction of the anti-CD44 S5 scFv has been described previously (Tan et al., 1995). The complete construct consists of the $V_L$ domain at the N-terminus linked to the $V_H$ domain at the C-terminus via a 15 amino acid linker $[Gly_4Ser]_3$. For the current studies, we first constructed the S5 scFv with an N-terminal histidine tag (His-tag) using the pET16b (Novagen, Madison, WI) expression plasmid vector. Subsequent binding studies, however, demonstrated that the N-terminal His-tag interfered with the antigen binding affinity. We then used polymerase chain reaction (PCR) mutagenesis techniques to introduce a C-terminal His-tag, and this scFv displayed an enzyme-linked immunosorbent assay (ELISA) $EC_{50}$ identical to that of the native scFv. All of the site-directed mutants have the same $His_6$ C-terminal extension, which allowed the production of highly pure scFv from *E. coli*. This gene was ligated into the pT7 Blue vector (Novagen) and used as a template for the site-directed mutagenesis manipulations.

Glutamine 44 was substituted with different amino acid residues by cassette mutagenesis. Sense (5′-CTG RH (R = A, G; H = A, C,T) G AAG CCA GGC CAG TCT CC-3′) and antisense (5′-CTT TGG AGA CTG GCC TGG CTT CDY (D = G, A, T; Y = C, T) CAG GTA C-3′) degenerate oligonucleotides were annealed and inserted into the scFv wild-type gene utilizing *Kpn*I and *Bsm*AI sites. The degenerate cassette produces changes to alanine, glutamic acid, lysine, methionine, threonine, and valine at position 44. The ligated vector was transformed into Novablue cells (Novagen), and the putative mutants were sequenced using dye terminator chemistry with fluorescence detection of the sequencing products (Applied Biosystem, Foster City, CA). Clones of interest were selected, and their inserts were ligated into the pET21a vector (Novagen) and subsequently transformed into BL21 (DE$\lambda$) for expression.

Because of lack of convenient restriction sites, glutamine 168 was substituted by PCR mutagenesis. A degenerate mutagenic sense primer (5′-CCA TGT CTT GGG TTC GCR HGA CTC CAG AAA AGA G-3′) was used in a first PCR reaction, together with a second antisense primer (5′-CCC GTC AAG CTT AGT GGT GAT GAT GGT GAT GTG AGG AGA CGG TTA CCG TGG TAC CTG C-3′) that coded for a stretch of six histidine residues and a *Hind*III site at the 3′ end. The extension of the primers was performed with Vent Polymerase (New England Biolabs). The primary PCR product was subsequently isolated and used in a second PCR step, together with a 5′ sense primer (5′-GGG AAT TCC ATA TGG AAG TGA AAC TGG TGG AGT CT-3′) carrying an *Nde*I site that sets the ATG start codon. In both steps, the wild-type scFv insert in pT7Blue was used as the template. The secondary PCR product was isolated and cut with *Nde*I and *Hind*III restriction enzymes, phenol/chloroform extracted, and ligated into *Nde*I and *Hind*III cut pUC18 vector. For screening purposes, an *Ear*I site near the mutated residue was removed in the mutagenic primer so that clones that do not have that *Ear*I site were likely to contain the desired mutagenic sequence alteration. Screened clones were selected and their DNA sequenced. Clones with the desired mutation were selected and the *Nde*I-*Hind*III insert ligated into pET21a and subsequently transformed into BL21 (DE$\lambda$).

Double mutants were constructed by cassette mutagenesis utilizing the two restriction sites, *Bsg*I and *Sac*I. The *Bsg*I site is located between positions 44 and 168, whereas the *Sac*I site is at the 3′ end of the gene. After ligation, the gene carrying double mutation was transformed into Novablue cells, screened by restriction mapping, and sequenced to select for clones of interest. ScFv insert from desired clones was ligated into pET21a and subsequently transformed into BL(DE$\lambda$). In all cases, the mutated genes in the pET21a vector were sequenced to confirm the presence of the desired mutation before expression.

### Expression of scFv mutants

The BL21(DE$\lambda$) cells containing the mutated scFv insert in the pET21a plasmid were grown overnight in 30 ml of Luria-Bertani (LB) medium supplemented with 100 $\mu$g/ml of ampicillin at 37°C with shaking. Cells were washed two times with 2× YT media the following day and used to

inoculate 6 liters of 2× YT media. When the $OD_{600}$ reached ~1.0, 0.2 mM isopropyl-b-D-thiogalactopyranoside (IPTG) was added to induce scFv expression. Cells were cultured for an additional 3 h and collected by spinning at 4500 × *g* for 10 min. The cell pellets were stored at −70°C before inclusion body isolation.

In each liter of induced culture, the cell pellet was resuspended in 30 ml of 50 mM Tris-HCl (pH 7.4), 8% sucrose, 3% Triton X-100, 300 mM NaCl, and 1 mM phenylmethylsulfonyl fluoride (PMSF). The cell suspension was sonicated, and the insoluble fractions consisting of inclusion bodies were centrifuged at 16,000 × *g* for 20 min. The insoluble fraction was washed three additional times. The inclusion bodies were sonicated each time to form a homogeneous suspension and centrifuged at 16,000 × *g* for 20 min. The inclusion bodies were then solubilized in 6 M guanidine-HCl, 100 mM $NaH_2PO_4$, and 10 mM Tris-HCl (pH 8.0) (binding buffer).

## Purification of scFv mutants

Ni-NTA resin was purchased from Qiagen (Chatsworth, CA) and used to pack a low-pressure 30-ml Econo-column (Biorad, Hercules, CA). The solubilized protein solution was passed over the column that had been preequilibrated with the binding buffer (see above). Fifteen column volumes of binding buffer were passed over the column to remove unbound protein, followed by 15 column volumes of washing buffer (6 M guanidine-HCl, 100 mM $NaH_2PO_4$, 0.5 M NaCl, 20 mM imidazole, 10 mM Tris-HCl, pH 6.3) to remove proteins that nonspecifically bound to the column. The bound protein was eluted using 6 M guanidine-HCl, 100 mM $NaH_2PO_4$, 0.5 M NaCl, 250 mM imidazole, and 10 mM Tris-HCl (pH 6.3). The eluted protein was precipitated by adding $(NH_4)_2SO_4$; washed two times with 50 mM Tris, 500 mM NaCl, and 2 mM mercaptoethanol; and resolubilized in 6 M guanidine-HCl to a final concentration of ~5–10 mg/ml, in preparation for refolding.

## Refolding of scFv mutants

The solubilized protein was diluted ~100-fold into a refolding buffer consisting of 50 mM 3-[cyclohexylamino]-1-propanesulfonic acid (CAPS) (pH 10.5), 0.35 M L-arginine, 0.1 mM PMSF, 2 mM EDTA, 1.25 mM cysteine, and 0.5 mM cystine that had been chilled to 4°C. The mixture was stirred for 1–2 h and left overnight at 4°C. On the following day, the protein solution was extensively dialyzed against 50 mM Tris-HCl (pH 7.5) and 150 mM NaCl that had been chilled to 4°C. The protein solution was then centrifuged to remove any insoluble materials and concentrated using an ultrafiltration cell (Amicon, Beverly, MA) to a volume of 3–10 ml. The refolded protein was then analyzed by sodium dodecyl sulfate-polyacrylamide gel electrophoresis (SDS-PAGE) to check its purity, which was 90–99%. Concentrations of scFv were determined by its absorbance at 280 nm, using an extinction coefficient of 53,403 $M^{-1}$ $cm^{-1}$ and a molecular weight of 27,427, which was calculated from the amino acid sequence of wild-type scFv.

## Chemical denaturation studies

A 7.2 M ultrapure guanidine-HCl solution in 50 mM Tris (pH 7.5) and 150 mM NaCl was prepared from 8 M guanidine-HCl solution (Fluka, Ronkonkoma, NY). The unfolding transition of each mutant was determined by monitoring changes in the intrinsic fluorescence maximum on a Hitachi spectrophotofluorometer F4500. A small volume (25 μl) of the 7.2 M guanidine-HCl solution was first added to a 40 μg/ml sample of each protein in 50 mM Tris (pH 7.5) and 150 mM NaCl. At each further addition, the sample was mixed and allowed to come to equilibrium. The optical chamber was thermostatted at 22°C in all of the measurements, which were performed in a 1 cm × 1 cm quartz fluorescence cuvette. The excitation wavelength was 290 nm, and the sample was scanned from 300 nm to 450 nm for each denaturant concentration. The fluorescence maximum was determined with a first-order derivative technique. There was a 14-nm red shift in fluorescence emission maximum upon denaturation of the scFv, and we estimate the accuracy of the determination of maximum wavelength of fluorescence emission to be 0.1–0.2 nm, based on analysis of standards and on the reproducibility of the data.

## Determination of $\Delta G_{n\text{-}u}$ and $m_G$ from the unfolding transitions

The Igor Pro (Lake Oswago, OR) software program was used to fit the unfolding transition, using a two-state protein unfolding model. The fitting equation is given below, which has been described by Santoro and Bolen (1988):

$$Y_{obs} = \frac{[(y_u^o + m_u[D]\{\exp[-(\Delta G_{n-u} - m_g[D])/RT]\} + (y_n^o + m_n[D])}{[\exp[-(\Delta G_{n-u} - m_g[D])/RT] + 1]}$$

The six fitting parameters are $y_n^o$ (minima), $m_n$ (pretransitional slope), $y_u^o$ (maxima), $m_u$ (posttransitional slope), $m_g$, and $\Delta G_{n\text{-}u}$ of unfolding and $Y_{obs}$ or $\lambda_{max}$ is the measured fluorescence maximum. $\Delta G_{n\text{-}u}$ is the Gibbs free energy of unfolding. The raw data ($\lambda_{max}$) for each unfolding transition was fit using the above equation. Each of the individual unfolding transitions for the mutant data sets was independently analyzed. The data sets for each mutant included a minimum of five individual unfolding experiments from at least two independent protein preparations. The average and standard deviation of $\Delta G_{n\text{-}u}$ and $m_g$ were then determined across each data set. The data was also fit to the three-state model, N → I → U. Assuming that the quantum yield of the three species are similar (which is true for N and U), the emission $\lambda_{max}$ should be directly related to the fraction of each species present according to the following equation (Barrick and Baldwin, 1993):

$$\lambda_{max,obs} = \lambda_{max,n} * F_n + \lambda_{max,i} * F_i + \lambda_{max,u} * F_u$$

$$F_n = \frac{1}{1 + K_{(n-i)} + K_{(n-i)} * K_{(i-u)}}$$

$$F_i = \frac{K_{(n-i)}}{1 + K_{(n-i)} + K_{(n-i)} * K_{(i-u)}}$$

$$F_u = 1 - F_n - F_i$$

This equation can be further manipulated to give

$$\lambda_{max,obs} = \frac{\lambda_{max,n} + \lambda_{max,i} * K(n-i) + \lambda_{max,u} * K(n-i) * K(i-u)}{1 + K(n-i) + K(n-i) * K(i-u)}$$

where

$$K_{(n-i)} = \exp((-\Delta G_{(n-i)} - m_g * D)/RT)$$

$$K_{(i-u)} = \exp((-\Delta G_{(i-u)} - m_g * D)/RT)$$

This nonlinear fitting equation involves seven fitting parameters, and the pre- and posttransitional baselines are assumed to be flat.

Equilibrium fluorescence data for selected mutants displaying significant $\Delta m_g$ and $\Delta\Delta G_{n\text{-}u}$ were also analyzed according to a two-state model using the numerically based program Bioeqs (Royer et al., 1990). Briefly, this solver uses a constraint optimization routine employing Lagrange mutlipliers to solve the free energy equation in terms of concentration of the chemical denaturant employed (Royer, 1993). The free energy equation used is $\Delta G_{obs} = \Delta G_{n\text{-}u} + m[\text{Gdn-HCl}]$. The pre- and posttransitional regions of the folding isotherm are assumed to be flat. The raw data ($\lambda_{max}$ versus denaturant concentration) were fitted to a two-state model using BIOEQS. Values for $m_g$, $\Delta G_{n\text{-}u}$, $y_n$ (minima), and $y_u$ (maxima) were generated from the BIOEQS fitting. The program also generated the

dependence of the $\chi^2$ minimum as a function of $\Delta G_{n\text{-}u}$ and $m_g$. The $\chi^2$ for the 67% confidence limit was determined using an extension program of the BIOEQS, allowing determination of the 67% confidence limit interval for $\Delta G_{n\text{-}u}$ and $m_g$.

## Determination of binding isotherm by competitive ELISA assay

Canine thyroid adenocarcinoma cells (CTACs) that display the CD44 antigen were plated onto 96 flat-bottom well plates and allowed to grow to confluency. The plates were washed two times with phosphate-buffered saline (PBS) plus 0.05% Tween 20. Cells in the plates were fixed using 0.15% glutaraldehyde for 30 min. The wells were washed three times with 0.05% Tween 20 in PBS, and the remaining binding sites in the wells were blocked by incubation with 100 $\mu$l of 5% nonfat milk in PBS for 30 min. Fifty microliters of scFv of varying concentrations (4 $\mu$M to $6 \times 10^{-2}$ nM) in PBS containing 2% bovine serum albumin was added to each well in duplicate, followed by an incubation of 30 min. A fixed amount of biotinylated parental antibody (S5) (50 $\mu$l of 3 nM protein) was added to each well and incubated for another 30 min. The wells were washed three times with Tween 20/PBS buffer. One hundred microliters of streptavidin-horseradish peroxidase (HRP) conjugate (Tagoimmunological, Camarillo, CA) was added to each well. After 30 min of incubation, the wells were washed three times as above, and 2,2′-azino-bis-3-ethylbenzthiazoline sulfonic acid (ABTS) substrate solution (Pierce, Rockford, IL) was added for color development. The optical density (OD) at 405 nm was measured after 15 min with a microtiter plate reader (Molecular Devices). The reading was blanked against wells in which no biotinylated S5 was added. The data were processed with the Igor software to determine the equivalent bulk concentration at 50% blocking of biotinylated S5 binding to the cells ($EC_{50}$), using a published four-parameter nonlinear fitting algorithm (Jin et al., 1992): $y = a + (d - a)/[1 + \exp(b(c - x))]$, where $a$, $b$, $c$, and $d$ are the adjustable fitting parameters, $x$ is the bulk antibody concentration ($\mu$M), and $y$ is the percentage block of biotinylated S5 binding. The $EC_{50}$ in $\mu$M is given by the value of the parameter $c$ for the best fit of the fitting function for the blocking isotherm.

## Quantitation of refolding yield

Proteins used for these studies were purified using the Nickel immobilized column as described in the above section. The guanidine-HCl-solubilized proteins were analyzed by SDS-PAGE and found to be homogeneous. Fifty micrograms of guanidine-HCl-solubilized protein was slowly dripped into 1 ml of refolding buffer consisting of 50 mM CAPS, 0.4 M L-arginine (pH 10.5), 1.25 mM cysteine, plus 0.5 mM cystine, and stirred overnight. The amount of solubilized protein was quantitated by measuring the $OD_{280}$, and subsequently dialyzed using a dialysis cassette (Pierce) against 50 mM Tris, 150 mM NaCl (pH 7.4) for 8 h. Protein samples were subsequently centrifuged at $10{,}000 \times g$ for 5 min. The concentration of protein at the endpoint of refolding was calculated by taking the $OD_{280}$ reading. The amount of protein was measured with a second independent method using the micro bicinchoninic acid (BCA) protein assay (Pierce). At the endpoint of refolding, 0.5 ml of BCA Protein assay reagent was added to 0.5 ml of each sample and incubated at 60°C for 1 h. The OD at 562 nm was then measured for each sample, and the amount of protein present was estimated from a standard curve generated using bovine serum albumin.

## Light scattering experiments

Fifty milligrams of guanidine-HCl-solubilized protein was added to 1 ml of 50 mM Tris, 150 mM NaCl, 1.25 mM cysteine, 0.5 mM cystine (pH 7.6). After rapid mixing, the light scattering of the sample was recorded over a 5-min (300-s) period at 22°C on a Hitachi F4500 fluorescence spectrophotometer with excitation and emission wavelength set at 500 nm.

# RESULTS

## Molecular modeling of the S5 scFv antibody structure

Our model single-chain antibody is the previously described S5 scFv (Tan et al., 1995), whose monoclonal parent stimulates a biochemical signaling cascade through the CD44 receptor that results in a remarkable increase in marrow graft acceptance between MHC mismatched donor/acceptor pairs (Sandmaier et al., 1990). The S5 scFv displays a close sequence homology to the crystallographically defined McPc603 antibody (Satow et al., 1986), with 67% exact match $V_H$ alignment (93% conservative match) and 69% exact match $V_L$ alignment (92% conservative match). Homology model building techniques were thus used to derive a three-dimensional model for S5. Fig. 1 *A* shows the overall fold of the scFv and the relationship of the $Gln^{44}$-$Gln^{168}$ interaction to the complementarity determining loops (CDR) and disulfide bonds. Fig. 1 *B* shows their relation-

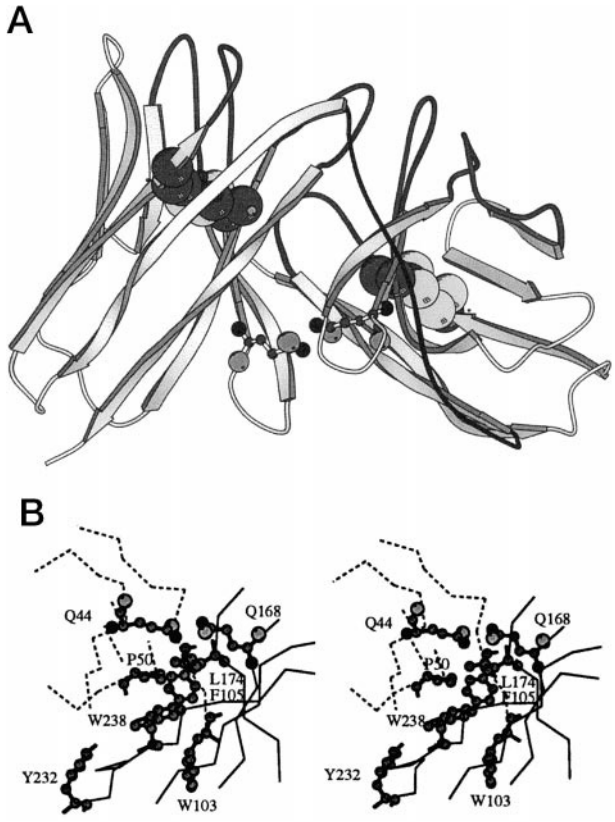


FIGURE 1 Homology three-dimensional model of the S5 scFv (MOLSCRIPT; Kraulis, 1991). (*A*) The S5 single-chain antibody with the $V_L$ domain on the left and $V_H$ domain on the right interconnected via a peptide linker (indicated by the *black coil*). The $Gln^{44}$-$Gln^{168}$ pair is shown as ball and stick, the CDR loops are represented by gray shading, and the two disulfide bonds are space filled. (*B*) Stereo view of the conserved $V_H$-$V_L$ interface. For $Gln^{44}$ and $Gln^{168}$, the medium-sized black ball represents the nitrogen atom and the large gray ball represents the oxygen atom. Six of the key residues involved in the $V_L$-$V_H$ packing are also shown as ball and stick, with all of the atoms colored gray. The $V_L$ central strands are shown as a dotted trace, and the $V_H$ central strands are shown as a solid trace.

ship to the conserved hydrophobic core residues (Chothia et al., 1985).

## Determination of $\Delta G_{n\text{-}u}$ and $m_g$

Chemical denaturation studies were used to determine the folding stability of the native S5 scFv and the site-directed mutants. These studies were conducted in the absence of reducing agents, and there are thus two disulfide links present in the folded and unfolded states. The unfolding transition was monitored by titrating the change in intrinsic fluorescence maximum as a function of denaturant concentration. There is a large red shift in the peak intrinsic fluorescence (14 nm) upon guanidinium denaturation, without a significant alteration in peak intensity (Fig. 2). This transition was fully reversible upon dilution back through the curve to zero denaturant concentration (data not shown). The scFv refolding is reversible through small chaotrope dilution steps once the correctly disulfide bonded and folded scFv is isolated. All of the unfolding curves shown in Fig. 3 represent averages of at least five independent experiments, generated from two independent antibody refolding and purification preparations. The $\Delta G_{n\text{-}u}$ and $m_g$ values were determined directly from the raw fluorescence data by nonlinear fitting using a two-state unfolding model (Santoro and Bolen, 1988), and significantly stabilized mutants were also analyzed with the BIOEQS fitting program (Royer, 1993). The data were described well with the two-state model, and application of a three-state model did not significantly improve the goodness of fit. The parameters recovered from these analyses and error estimates are reported in Tables 1 and 2. Although the results in these tables were obtained from direct fitting of the raw data, we have plotted the unfolding isotherms on the percentage unfolded axis in Fig. 3 for easier comparison of the mutants. As previously discussed, these absolute values should be viewed cautiously (Santoro and Bolen, 1988). The relative $\Delta\Delta G_{n\text{-}u}$ and $\Delta m_g$ are generally quite accurate and provide a reliable index for comparing the native S5 scFv and the site-directed mutants (Matouschek et al., 1994).

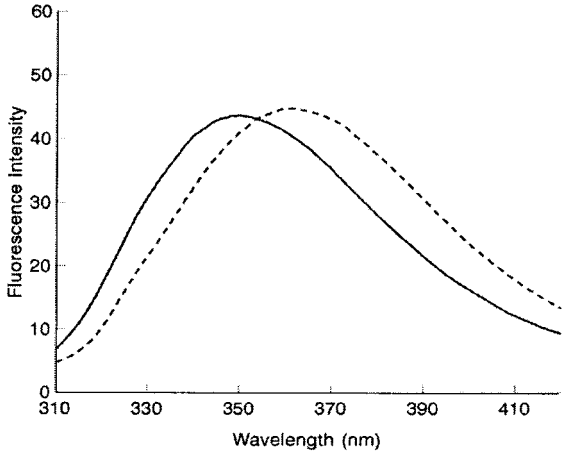


FIGURE 2 Fluorescence emission spectra for the folded scFv (50 mM Tris, pH 7.5, 150 mM NaCl) and the GnCl-denatured S5 scFv scFv (50 mM Tris, pH 7.5, 150 mM NaCl, 6 M Gn-HCl). Protein concentration was 0.4 $\mu$M and sample excitation was at 290 nm.

### *Ala double mutant cycle*

Removing the two hydrogen bonds between $Gln^{44}$ and $Gln^{168}$ by sequentially substituting alanine across the interface has little effect on the unfolding free energy (Table 1). The Q168A and Q44A/Q168A mutations slightly reduce the stability of the scFv without significantly altering the $m_g$, whereas the Q44A mutation results in a small increase in the folding stability (Fig. 3 *A*).

### *Met double mutant cycle*

In an attempt to bury more surface area at the $V_H/V_L$ interface, we constructed a series of mutants with methionine introduced in different permutations at $Gln^{44}$ and/or $Gln^{168}$. In the first set, a double mutant cycle was constructed with the native $Gln^{44}/Gln^{168}$. Each of the two single mutants, Q44M/Q168 and Q44/Q168M, displayed significant increases in the $m_g$ value and the folding free energy (Table 1 and Fig. 3 *B*). The double mutant Q44M/Q168M displayed an unfolding transition with an $m_g$ essentially identical to the native scFv and an increase in stability via a small shift in $C_m$.

### *Ala/Met double mutant cycle*

A double mutant cycle was also constructed between the double alanine and double methionine mutants, to potentially provide a better steric fit in the folded state for the single methionine mutants. As previously noted, the Q44A/Q168A displays $m_g$ and $\Delta\Delta G_{n\text{-}u}$ values essentially identical to those of the wild type, whereas the Q44M/Q168M double mutant displays a $\Delta\Delta G_{n\text{-}u}$ of 0.5 kcal/mol. Both the Q44A/Q168M and Q44M/Q168A mutants display large increases in $m_g$ and $\Delta G_{n\text{-}u}$ (Table 1 and Fig. 3 *C*). The Q44A/Q168M mutant displays an unfolding isotherm that is more stable with respect to the denaturant concentration where unfolding is initiated, and then displays a sharply cooperative transition to the denatured state. The transition is steeper than the Q168M single mutant, and displays a significantly increased initial resistance to denaturation. The Q44M/Q168A isotherm is within experimental error of the Q44M/Q168 single mutant isotherm.

### *Glu/Lys double mutant cycles*

Double mutant cycles introducing Lys and Glu at positions 44 and 168 were constructed in both directions across the interface. The mutations in the Q44E/Q168K cycle had little effect on the folding stability (Table 1 and Fig. 3 *D*), with the Q44E and Q168K single mutants displaying $\Delta G_{n\text{-}u}$ and $m_g$ values essentially within experimental error of the native

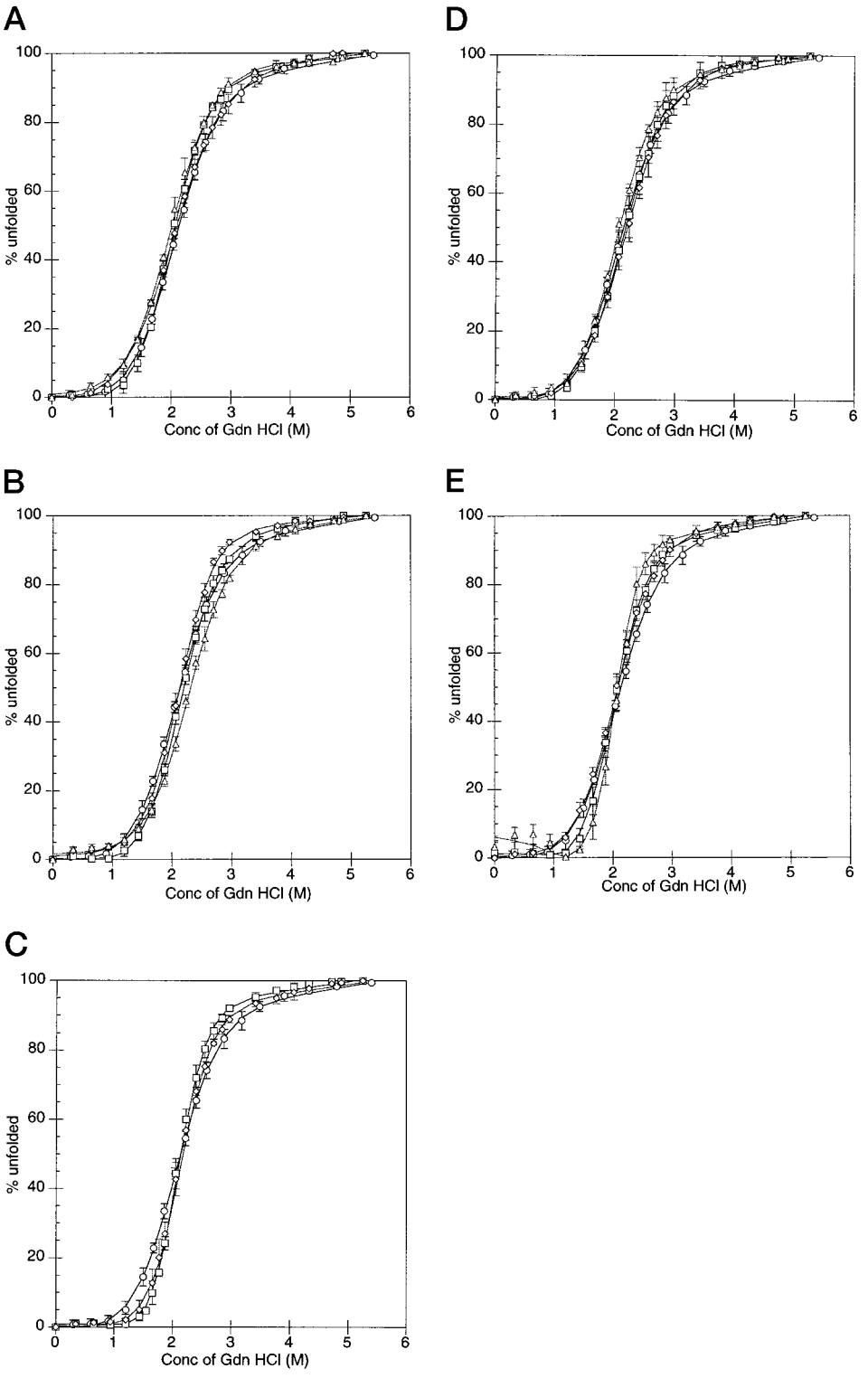


FIGURE 3 Guanidine-HCl unfolding titrations for the native scFv and Q44/Q168 site-directed mutants plotted on the percentage unfolded scale for visual comparison. The data points, with standard deviations, represent averages of at least five unfolding experiments from a minimum of two independent protein preparations. The solid lines represent the nonlinear fits to the two-state folding model. (*A*) Native scFv (○), Q44A (□), Q168A (◇), Q44A/Q168A (△). (*B*) Native scFv (○), Q44M (□), Q168M (◇), Q44M/Q168M (△). (*C*) Native scFv (○), Q44A/Q168M (□), Q44M Q168A (◇). (*D*) Native scFv (○), Q44E (□), Q168K (◇), Q44E/Q168K (△). (*E*) Native scFv (○), Q44K (□), Q168E (◇), Q44K/Q168E (△).

antibody. The Q44E/Q168K double mutant was slightly stabilized relative to wild type, with a small increase in the $m_g$ value. The second cycle, with the salt-bridge polarity reversed, did display significant alterations (Fig. 3 *E*). Whereas the Q168E mutant was within experimental error of the native isotherm, the Q44K single mutant displayed a significantly larger and more positive $m_g$ and a corresponding increase in $\Delta\Delta G_{n\text{-}u}$ of ~1 kcal/mol. The Q44K/Q168E double mutant displayed an even larger increase in $m_g$ and a $\Delta\Delta G_{n\text{-}u}$ of ~2 kcal/mol. There was a small but reproducible fluorescence emission transition at low denaturant concentrations with this mutant, which we have assigned to a local interface effect that is distinct from global folding. Some uncertainty in the $m_g$ and $\Delta\Delta G_{n\text{-}u}$ values is introduced by this transition, as the pretransition slope cannot be accurately determined.

**TABLE 1A $\Delta G_{n-u}$ and $m_g$ for alanine and methionine mutants**

| Proteins | $\Delta G^*_{n-u}$ (kcal/mol) | $m^*_g$ (kcal/mol/M) |
|---|---|---|
| wt | 3.20 ± 0.12 | 1.57 ± 0.04 |
| Q44M | 3.93 ± 0.08 | 1.90 ± 0.02 |
| Q168M | 4.04 ± 0.23 | 1.97 ± 0.14 |
| Q44M Q168M | 3.70 ± 0.04 | 1.64 ± 0.04 |
| Q44A | 3.76 ± 0.13 | 1.90 ± 0.08 |
| Q168A | 2.86 ± 0.09 | 1.48 ± 0.10 |
| Q44A Q168A | 3.13 ± 0.09 | 1.58 ± 0.06 |
| Q44A Q168M | 4.67 ± 0.11 | 2.22 ± 0.11 |
| Q44M Q168A | 4.50 ± 0.26 | 2.20 ± 0.13 |

Data given are mean ± SD.

## Double mutant cycle analyses

Double mutant cycles were constructed from the unfolding free energies and are summarized in Fig. 4. There are relatively large interaction free energies of 1.1, 2.4, and −0.8 kcal/mol observed for the methionine, methionine/alanine, and $Lys^{44}/Glu^{168}$ complementary charge cycles, respectively.

## $EC_{50}$ determinations of binding activities

The S5 scFv was previously shown to retain the CD-44 binding affinity of its Fab′ counterpart in an ELISA-based $EC_{50}$ assay (Tan et al., 1995). The C-terminal histidine tag construct used in this study displayed an equivalent $EC_{50}$ value when compared to the original construct. The $EC_{50}$ values for the mutants are summarized in Table 3. The binding affinity for all mutants was reduced relative to wild type. The Q44A/Q168M and Q44M/Q168A mutants were least affected with a relative $EC_{50}$ of ~2.5. With the exception of the double alanine mutant, the others have relative $EC_{50}$'s that range from 3.0 to 4.5. The Q44A/Q168A mutant displays the largest alteration, with a relative $EC_{50}$ value of 8.0. Because these assays are conducted with washing steps in a concentration range that is close to the expected $K_a$, the alterations in $EC_{50}$ could reflect changes in $k_{off}$ and are likely to represent relatively small alterations on the binding free energy scale.

**TABLE 1B $\Delta G_{n-u}$ and $m_g$ for salt bridge mutants**

| Proteins | $\Delta G^*_{n-u}$ (kcal/mol) | $m^*_g$ (kcal/mol/M) |
|---|---|---|
| wt | 3.20 ± 0.12 | 1.57 ± 0.04 |
| Q44E | 3.33 ± 0.20 | 1.56 ± 0.06 |
| Q168K | 3.30 ± 0.07 | 1.55 ± 0.04 |
| Q44E Q168K | 3.73 ± 0.11 | 1.87 ± 0.05 |
| Q44K | 4.15 ± 0.21 | 2.10 ± 0.14 |
| Q168E | 3.53 ± 0.32 | 1.78 ± 0.21 |
| Q44K Q168E | 5.30 ± 0.20 | 2.65 ± 0.10 |

Data given are mean ± SD.

**TABLE 2 $\Delta G_{n-u}$ and $m_g$ for selected mutants as analyzed by BIOEQS**

| Proteins | $\Delta G^*_{n-u}$ (kcal/mol) | $m^*_g$ (kcal/mol/M) |
|---|---|---|
| wt | 3.00 [2.74, 3.28] | 1.42 [1.29, 1.55] |
| Q44A Q168M | 4.70 [4.42, 5.03] | 2.21 [1.97, 2.52] |
| Q44M Q168A | 4.76 [4.30, 5.29] | 2.22 [2.01, 2.47] |
| Q44K Q168E | 5.0 [4.00, 6.50] | 2.23 [1.80, 2.90] |

Data given are mean with 67% confidence limit in [ ].

## Refolding efficiency studies

Table 4 summarizes the refolding efficiencies observed with selected scFv interface mutants. The refolding of the scFv in a redox buffer by rapid dilution to nondenaturing conditions is not reversible, as distinct from the reversibility observed upon small denaturant dilution steps with a correctly disulfide-bonded scFv. The data represented an average of four to six independent refolding experiments. Two independent methods of measuring the refolding efficiency were utilized, and the $OD_{280}$ and micro BCA protein assay results were in excellent agreement. The refolding efficiency of wild type is ~10%, whereas that of the single methionine mutants (Q44M and Q168M) is ~20–27%. The double methionine mutant did not produce an additive effect. The double alanine/methionine mutants also displayed an increase in refolding efficiency, with the Q44A Q168M increasing the refolding efficiency to 21%. The Q44E/Q168K and Q44K/Q168E mutants displayed little or no increase in refolding efficiency. The Q44A Q168A mutant displayed a modest increase over the wild type. The aggregation behav-

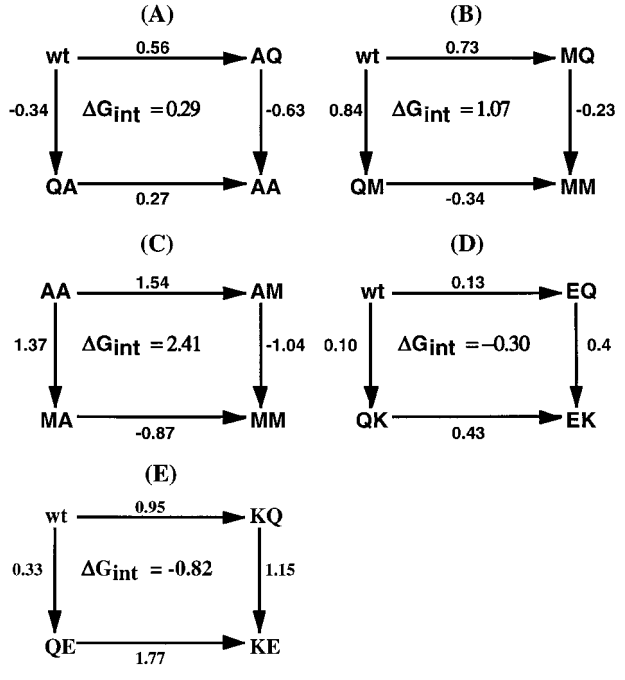


FIGURE 4 Double mutant cycle analyses at $Gln^{44}/Gln^{168}$. The numerical values represent the unfolding free energies in kcal/mol as recovered from the analyses reported in Table 1.

**TABLE 3 $EC_{50}$ data from competitive ELISA binding assays**

| Proteins | $EC_{50}$ (nM) |
|---|---|
| wt | 0.18 ± 0.01 |
| Q44M | 0.80 ± 0.15 |
| Q168M | 0.73 ± 0.07 |
| Q44M Q168M | 0.71 ± 0.05 |
| Q44A | 0.61 ± 0.02 |
| Q168A | 0.87 ± 0.01 |
| Q44A Q168A | 1.59 ± 0.30 |
| Q44A Q168M | 0.45 ± 0.04 |
| Q44M Q168A | 0.47 ± 0.02 |
| Q44K Q168E | 0.67 ± 0.08 |
| Q44E Q168K | 0.75 ± 0.05 |

ior of selected mutants over a period of 300 s after the initiation of protein refolding is shown in Fig. 5. Most of the aggregation kinetic pathway is complete during the mixing time of 3–4 s. The wild-type scFv displays the highest aggregation, as indicated by the scattering intensity at 500, and the double methionine mutant (Q44M and Q168M) displays the lowest level of aggregation. Table 4 summarizes these results.

## DISCUSSION

The apparent two-state $V_H$-$V_L$ assembly process implies significant thermodynamic coupling and cooperativity between the folding and association equilibria. Because the scFv antibodies are not found in nature, evolutionary pressure has optimized the $V_H$-$V_L$ interface in the context of the closely associated $C_{H1}$-$C_L$ interface. The mutants that display higher folding free energy also display a loss of binding free energy, suggesting that the interface is designed to architecturally optimize antigen recognition rather than thermodynamic folding stability. The $C_{H1}$-$C_L$ domains and interface are coupled to $V_H$-$V_L$ folding and serve as stabilizing domains, with the $V_H$-$V_L$ interface (not just the complementarity determining loops) properly viewed as an extension of the "active site" of IgG antibodies. Fersht and Matthews have previously pointed out that there is no

**TABLE 4 Refolding efficiency of wild-type and hydrogen-bonding mutants**

| Proteins | Refolding efficiency* | Refolding efficiency# |
|---|---|---|
| wt | 9.3 ± 2.8 | 8 ± 3.9 |
| Q44M | 22.4 ± 5.0 | 19.5 ± 5.7 |
| Q168M | 27 ± 3.4 | 21.2 ± 4.8 |
| Q44M Q168M | 25.5 ± 6.0 | 26.2 ± 6.0 |
| Q44A Q168M | 21.8 ± 6.0 | 20.3 ± 6.9 |
| Q44M Q168A | 15.3 ± 3.8 | 17.7 ± 6.2 |
| Q44A Q168A | 14.5 ± 3.7 | 13 ± 6.0 |
| Q44E Q168K | 15.7 ± 4.4 | 12.5 ± 4.6 |
| Q44K Q168E | 12.6 ± 3.8 | 9.9 ± 4.5 |

*Refolding efficiency determined by $OD_{280}$ quantitation.
#Refolding efficiency determined by BCA measurements.

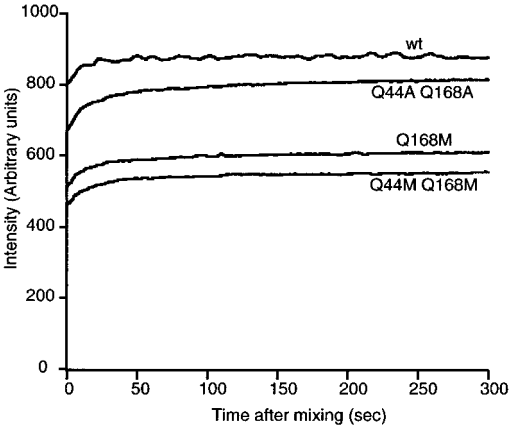


FIGURE 5 Light scattering measurements of the aggregation kinetics of scFv hydrogen bonding mutants. The experimental conditions are described in Materials and Methods.

reason to expect that residues providing key functional roles in enzymes have also been simultaneously selected for folding fitness (Schreiber et al., 1994; Shoichet et al., 1995).

A key finding is that despite being remarkably conserved throughout the IgG antibody family, the $Gln^{44}$-$Gln^{168}$ interaction is not important to scFv folding stability. The Q44A, Q168A, and Q44A/Q168A mutants display only very small alterations in stability that are close to the error limits of our measurements. In addition to studying the effects of hydrogen bond removal, we were interested in testing whether the hydrophobic interfacial core could be extended by engineering methionine side chains at $Gln^{44}$ and $Gln^{168}$. Several mutants display stability increases that are relatively large. Whereas the double Q44M/Q168M mutant displayed an apparently conventional increase in $\Delta\Delta G_{n\text{-}u}$ of ~0.5 kcal/mol with constant $m_g$, all of the single methionine mutants with glutamine or alanine at the complementary position displayed corresponding positive increases in $\Delta m_g$ and $\Delta\Delta G_{n\text{-}u}$. With the Q168M mutants, there was significant benefit to having the smaller alanine side chain at position 44, with an approximate doubling of $+\Delta m_g$ and $\Delta\Delta G_{n\text{-}u}$ with Q44A/Q168M relative to Q44/Q168M. The interaction free energies shown in Fig. 4 must therefore be interpreted cautiously and may reflect interactions in the unfolded state as well as the folded state.

The effects of introducing complementary full charges at $Gln^{44}$ and $Gln^{168}$ were strongly dependent on their directionality across the interface. The Q44E/Q168K orientation had only a small stabilizing effect, with a correspondingly small $m_g$ alteration. However, the Q44K/Q168E mutant displayed a large positive change in $\Delta m_g$ and $\Delta\Delta G_{n\text{-}u}$. The strong directionality dependence of the complementary charge mutants is likely to involve a local electrostatic effect, as calculations have suggested that the $V_H$ has a mostly negative surface potential and the $V_L$ a complementary positive potential (Getzoff et al., 1986). Lysine has polar (48 $Å^2$) and nonpolar (119 $Å^2$) side-chain surface areas very similar to those of methionine (43 and 117 $Å^2$, respectively), and the burial of methylene surfaces at the

interface could also play an important role in the stabilization of the $V_H/V_L$ association, or have significant effects on the unfolded states.

Rowe has pointed out that the unfolding of two antibody domains connected by a covalent linker can be described as the product of a pseudodissociation constant and the equilibrium constants for the unfolding of the two individual domains (1976):

$$K_{n-u} = K_d' K_{VH} K_{VL}$$

where $K_{n\text{-}u}$ is the equilibrium constant for the unfolding of the scFv, $K_d'$ is the unimolecular $V_H$-$V_L$ dissociation constant, and $K_{VH}/K_{VL}$ are the equilibrium constants for the unfolding of the individual $V_H$ and $V_L$ subunits. A schematic model of this unfolding scheme, which has also been used by Pantoliano and co-workers in the context of scFv stability (1991), is shown in Fig. 6. Brandts has developed an explicit derivation of its consequences to examine the calorimetric deconvolution of interacting folding domains (1989). At one limit is the strong coupling case, in which the association is tight and a higher concentration of denaturant is required to unfold the protein than is required for unfolding the isolated domains. The association energy keeps the subunits folded at a denaturant concentration where they would normally be unfolded. In the weak coupling limit, the domain unfolding occurs at a significantly higher denaturant concentration than dissociation, so that the observed unfolding titration is largely a function of the relative properties of the isolated subunits.

If the altered subunit interface results in a higher association free energy (smaller $K_d'$), then the initiation of unfolding could be shifted to higher denaturant concentrations. The coupling between association and unfolding is more closely linked, and the increase in association energy results in an increase in $m_g$. The $m_g$ term in chemical denaturation studies has previously been related to $\Delta A_{n\text{-}u}$ (Shortle and Meeker, 1986; Shortle, 1995; Myers et al., 1995). The site-directed mutation(s) could thus also give rise to a $+\Delta m_g$ via an increase in the surface area of the unfolded state (with $K_{VH}$ and/or $K_{VL}$ altered by a shift in the free energy of the unfolded state). The scFv have one disulfide bond in each of $V_H$ and $V_L$ domains, and these are likely to impart a degree of structure in the unfolded state (Myers et al., 1995). Some of the mutations could further disrupt this vestigial structure toward a more solvent-accessible, extended state.

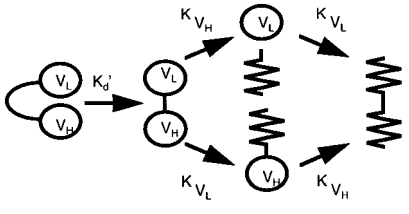


FIGURE 6 Schematic model for the unfolding of scFv as adapted from Rowe (1976).

Another principal means by which mutations could result in $\Delta m_g$ is under conditions where the two-state assumption is altered. It is often experimentally difficult to distinguish whether an equilibrium denaturation curve reflects small accumulations of folding intermediates because of data fitting uncertainties, and a $+\Delta m_g$ could reflect a shift toward higher cooperativity and true two-state behavior (or vice versa). This could arise in the context of Fig. 6 when the wild-type association free energy is relatively small, and the system is not completely coupled to a two-state equilibrium. Our use of a three-state fitting model did not result in a better fit to the unfolding data, but we cannot rule out this possibility.

A significant limitation with the production of many scFv is poor refolding efficiency. The low refolding yield is often attributed to the irreversible side reactions, such as protein aggregation (Jaenicke, 1887; London et al., 1974; Zettlmeissl et al., 1979). Pluckthun and co-workers have reported that mutations in the framework region of a single-chain Fv greatly reduced aggregation and improved refolding yield (Knappick and Pluckthun, 1995). We checked to see whether any of the S5 scFv mutants had altered refolding efficiencies to probe the role of $V_H/V_L$ interface in the refolding pathway and to see if thermodynamic stability was correlated with refolding efficiency. We used the reduced scFv as a starting point, whereas Knappick and Pluckthun utilized disulfide-intact scFv. There were significant alterations in the refolding efficiencies, as summarized in Table 4. There was not a correlation between aggregation and thermodynamic stabilities. This suggests that it is indeed a kinetic step that is being altered by the $V_H/V_L$ interface mutations, such as an increase in the rate of native refolding or a decrease in the committed rate controlling the aggregation partition. The finding that $V_H/V_L$ interface mutations can significantly increase refolding efficiencies could provide a new avenue for optimizing production strategies.

## CONCLUSIONS

There are three primary mechanisms available for increasing the thermodynamic stability of scFv antibodies: 1) increase the $V_H/V_L$ association free energy, 2) destabilize the scFv unfolded state, or 3) increase the stability of isolated $V_H$ and/or $V_L$ domains. Several of the $Gln^{44}/Gln^{168}$ mutants display significantly increased $m_g$ and $\Delta G_{n\text{-}u}$ values, which we have qualitatively interpreted as being due to an increase in the $V_H/V_L$ association free energy and/or a perturbation of the scFv unfolded state. The effect of improving $V_H/V_L$ interactions can be described as an increase in cooperativity, where the increased association free energy keeps the $V_H$ and $V_L$ folded at denaturant concentrations at which the isolated domains would be unfolded. Although the $V_H/V_L$ interface mutations reduce the antigen binding affinity to a small extent, these studies suggest that reengineering of the $V_H/V_L$ interface may thus provide new avenues for improving scFv stability and refolding efficiency.

We gratefully acknowledge the research support provided by The Whitaker Foundation for this work, Dr. John Hill for his assistance with the BIOEQS program, and Erlinda Santos for her technical assistance in the cell culture work.

## REFERENCES


Barrick, D., and R. L. Baldwin. 1993. Three-state analysis of sperm whale apomyoglobin folding. *Biochemistry.* 32:3790–3796.

Bird, R. E., K. D. Hardman, J. W. Jacobson, S. Johnson, B. M. Kaufman, S-M. Lee, T. Lee, S. H. Pope, G. S. Riordan, and M. Whitlow. 1988. Single-chain antigen-binding proteins. *Science.* 242:423–426.

Brandts, J. F., C. Q. Hu, and L-N. Lin. 1989. A simple model for proteins with interacting domains. Applications to scanning calorimetry data. *Biochemistry.* 28:8588–8596.

Chothia, C., and A. M. Lesk. 1986. Relationship between the divergence of sequence and structure in proteins. *EMBO J.* 5:823–826.

Chothia, C., J. Novotny, R. Bruccoleri, and M. Karplus. 1985. Domain association in immunoglobulin molecules—the packing of variable domains. *J. Mol. Biol.* 186:651–663.

Freund, C., A. Honegger, P. Hunziker, T. A. Holak, and A. Pluckthun. 1996. Folding nuclei of the scFv fragment of an antibody. *Biochemistry.* 35:8457–8464.

Getzoff, E. D., J. A. Tainer, and A. J. Olson. 1986. Recognition and interactions controlling the assemblies of $\beta$ barrel domains. *Biophys. J.* 49:191–206.

Glockshuber, R., M. Malia, I. Pfitzinger, and A. Pluckthun. 1990. A comparison of strategies to stabilize immunglobulin Fv-fragments. *Biochemistry.* 29:1362–1367.

Gulliver, G. A., C. A. Rumbley, J. Carrero, and E. W. Voss. 1995. Relative conformational stabilities of single-chain pocket and groove-shaped antibody active sites including HCDR transplant intermediates. *Biochemistry.* 34:5158–5163.

Hochman, J., M. Gavish, D. Inbar, and D. Givol. 1976. Folding and interaction of subunits at the antibody combining site. *Biochemistry.* 15:2706–2710.

Horne, C., M. Klein, I. Polidoulis, and K. J. Dorrington. 1982. Noncovalent association of heavy and light chains of human immunoglobulins. III. Specific interactions between $V_H$ and $V_L$. *J. Immunol.* 129:660–665.

Jaenicke, R. 1987. Folding and association of proteins. *Prog. Biophys. Mol. Biol.* 49:117–237.

Jin, L., B. M. Fendly, and J. A. Wells. 1992. High resolution functional analysis of antibody-antigen interactions. *J. Mol. Biol.* 226:851–865.

Kabat, E. A., T. T. Wu, H. M. Perry, K. S. Gottesman, and C. Foeller. 1991. Sequences of Proteins of Immunological Interest. National Institute of Health, Bethesda, MD.

Klein, M., C. Kortan, D. I. C. Kells, and K. J. Dorrington. 1979. Equilibrium and kinetic aspects of the interaction of isolated variable and constant domains of light chain with the Fd′ fragment of immunoglobulin G. *Biochemistry.* 18:1473–1481.

Knappick, A., and A. Pluckthun. 1995. Engineered turns of a recombinant antibody improve its in vivo folding. *Protein Eng.* 8:81–89.

Kraulis, P. J. 1991. MOLSCRIPT. A program to produce both detailed and schematic plots of protein structures. *J. Appl. Crystallogr.* 24:946–950.

Lilie, H., R. Jaenicke, and J. Buchner. 1995. Characterization of a quaternary-structured folding intermediate of an antibody Fab-fragment. *Protein Sci.* 4:917–924.

London, J., C. Skrzynia, and M. E. Goldberg. 1974. Renaturation of *Escherichia coli* tryptophanase after exposure to 8 M urea. Evidence for the existence of nucleation centers. *Eur. J. Biochem.* 47:409–415.

Matouschek, A., J. M. Matthews, C. M. Johnson, and A. Fersht. 1994. Extrapolation to water of kinetic and equilibrium data for the unfolding of barnase in urea solutions. *Protein Eng.* 7:1089–1095.

Myers, J. K., C. N. Pace, and J. M. Scholtz. 1995. Denaturant m values and heat capacity changes: relation to changes in accessible surface areas of protein folding. *Protein Sci.* 4:2138–2148.

Neet, K. E., and D. E. Timm. 1994. Conformational stability of dimeric proteins: quantitative studies by equilibrium denaturation. *Protein Sci.* 3:2167–2174.

Pantoliano, M. W., R. E. Bird, S. Johnson, E. D. Asel, S. W. Dodd, J. F. Wood, and K. D. Hardman. 1991. Conformational stability, folding and ligand-binding affinity of single-chain Fv immunoglobulin fragments expressed *Escherichia coli*. *Biochemistry.* 30:10117–10125.

Reiter, Y., U. Brinkmann, R. J. Kreitman, S-H. Jung, B. Lee, and I. Pastan. 1994. Stabilization of the Fv fragments in recombinant immunotoxins by disulfide bonds engineered into conserved framework regions. *Biochemistry.* 33:5451–5459.

Rowe, E. S. 1976. Dissociation, and denaturation equilibria, and kinetics of a homogeneous human immunoglobulin Fab fragment. *Biochemistry.* 15:905–916.

Rowe, E. S., and C. Tanford. 1973. Equilibrium and kinetics of the denaturation of a homogeneous human immunoglobulin light chain. *Biochemistry.* 12:4822–4827.

Royer, C. A. 1993. Improvements in the numerical analysis of thermodynamic data from biomolecular complexes. *Anal. Biochem.* 210:91–97.

Royer, C. A., W. R. Smith, and J. M. Beechem. 1990. Analysis of binding in macromolecular complexes: a generalized numerical approach. *Anal. Biochem.* 191:287–294.

Sandmaier, B. M., R. Storb, F. R. Appelbaum, and W. M. Gallatin. 1990. An antibody that facilitates hematopoietic engraftment recognizes CD44. *Blood.* 76:630–635.

Santoro, M. M., and D. W. Bolen. 1988. Unfolding free energy changes determined by the linear extrapolation method. 1. Unfolding of phenylmethanesulfonyl a-chymotrypsin using different denaturants. *Biochemistry.* 27:8069–8074.

Satow, Y., G. H. Cohen, E. A. Padlan, and D. R. Davies. 1986. Phosphocholine binding to immunoglobulin Fab McPC603. An x-ray diffraction study at 2.7 Å. *J. Mol. Biol.* 190:593–604.

Sauer, R. T., Milla, M. E., Waldburger, C. D., Brown, B. M., and Schildbach, J. F. 1996. Sequence determinants of folding and stability for the P22 Arc repressor dimer. FASEB J. 10:42–48.

Schreiber, G., A. M. Buckle, and A. R. Fersht. 1994. Stability and function: two constraints in the evolution of barstar and other proteins. *Curr. Biol.* 2:935–951.

Shoichet, B. K., W. A. Baase, R. Kuroki, and B. W. Matthews. 1995. A relationship between protein stability and protein function. *Proc. Natl. Acad. Sci. USA.* 92:452–456.

Shortle, D. 1995. Staphylococcal nuclease: a showcase of m-value effects. *Adv. Protein Chem.* 46:217–247.

Shortle, D., and A. K. Meeker. 1986. Mutant forms of staphylococcal nuclease with altered patterns of guanidine hydrochloride and urea denaturation. *Proteins Struct. Funct. Genet.* 1:81–89.

Tan, P. H., B. M. Sandmaier, and P. S. Stayton. 1995. Characterization of an anti-CD44 single-chain Fv antibody that stimulates natural killer cell activity and induces TNF$\alpha$ release. *Immunol. Invest.* 24:907–926.

Tsunenaga, M., Y. Goto, Y. Kawata, and K. Hamaguchi. 1987. Unfolding and refolding of a type k immunoglobulin light chain and its variable and constant fragments. *Biochemistry.* 26:6044–6051.

Zettlmeissl, G., R. Rudolph, and R. Jaenicke. 1979. Reconstitution of lactic dehydrogenase. Noncovalent aggregation vs. reactivation. 1. Physical properties and kinetics of aggregation. *Biochemistry.* 18:5567–5571.